

Cite this: DOI: 10.1039/xxxxxxxxxx

## Precise measurements of capsule mechanical properties using indentation<sup>†</sup>

 Joseph D. Berry,<sup>\*ab‡</sup> Srinivas Mettu,<sup>ab</sup> and Raymond R. Dagastine<sup>ab¶</sup>

 Received Date  
Accepted Date

DOI: 10.1039/xxxxxxxxxx

www.rsc.org/journalname

**Application of elastic theory to experimental data of capsule and particle compression under-predicts the value of material properties such as the Young's modulus by up to 100% when the effect of the rigid substrate is neglected, as is commonly done in the literature. Results of numerical simulations, spanning the range from thin-shelled capsules to solid particles, are presented in terms of correction factors that account for the substrate. In addition, the scaling relationship between indentation force and displacement is characterised for arbitrary shell thicknesses and indenter radii.**

The elasticity of materials is of fundamental importance to a wide range of engineering applications. The resistance of a material to elastic deformation is known as the “Young's modulus”, denoted by  $E$ , a quantity defined in the 18th century by Euler and first used experimentally by Riccati in 1782<sup>1</sup>. A common repeatable and non-destructive method of determining the Young's modulus of materials is the indentation test<sup>2,3</sup>, whereby the material is subjected to a prescribed load, the subsequent indenter displacement is measured, and  $E$  is calculated from the force-indentation data. Indentation of  $O(\text{mm})$  thick films is carried out by macroscale indenters. However, with miniaturization of technologies, the need for controlled indentation of micron-scale objects such as particles and capsules has arisen.

Atomic Force Microscopy (AFM) has been used with great success to measure the moduli of microscale objects<sup>4,5</sup>. Cells<sup>6</sup>, microparticles<sup>7</sup>, or microcapsules<sup>8</sup> are indented by a distance of nanometres using either nano-indenters, colloidal probes, or AFM

cantilever tips to determine material properties. This type of measurement is of fundamental importance in many biological, pharmaceutical, personal-care products and food processing applications. Accurate measurements of stiffness are crucial to determine if drug-delivery capsules are bio-compatible, or to define robustness in various processes associated with pressure sensitive adhesives, fragrance or flavour delivery and newer technologies such as self healing materials<sup>9</sup>. In particular, stiffness has been correlated to the disease state of a cell<sup>10</sup> and cells have been shown to be extremely sensitive to the stiffness, and hence the modulus, of materials<sup>11,12</sup>. Further, softer particles have been shown to be able to circulate longer within the bloodstream, due to their ability to deform through narrow vessels, and also evade immune system phagocytosis more effectively than stiffer particles<sup>13</sup>.

In most cases, calculation of the stiffness and associated elastic moduli of thin-shelled micro-capsules and particles is analysed using the theory of Reissner<sup>14</sup>. and Hertz<sup>15</sup> respectively. For a given indentation  $\delta$  (less than the shell thickness  $h$ ), the force  $F$  on a thin shell capsule of radius  $R$ , Young's modulus  $E$  and Poisson's ratio  $\nu$  is defined using Reissner's formula as

$$F = \frac{4Eh^2\delta}{R\sqrt{3(1-\nu^2)}} \quad (1)$$

The application of Equation 1 is appropriate for capsules with shell thickness ratio  $h/R < 1/20$ <sup>16</sup>. Similarly, the force on a particle as a function of (small) applied indentation was defined by Hertz in 1882 as

$$F = \frac{4E\bar{R}^{\frac{1}{2}}\delta^{\frac{3}{2}}}{3(1-\nu^2)} \quad (2)$$

Here  $\bar{R} = R_p R / (R_p + R)$  is the effective radius of the probe radius  $R_p$  and the particle radius  $R$ . Equation 2 is valid when the Young's modulus of the indenter  $E_p$  is much greater than  $E$ , otherwise the effective Young's modulus must be used<sup>17</sup>.

Almost all analysis of experimental force-indentation data conducted in the literature neglects to account for the indentation of the particle or capsule due to the presence of the solid sub-

<sup>a</sup> Department of Chemical & Biomolecular Engineering, University of Melbourne, Parkville, Victoria 3010, Australia

<sup>b</sup> Particulate Fluids Processing Centre, University of Melbourne, Parkville, Victoria 3010, Australia

<sup>†</sup> Electronic Supplementary Information (ESI) available: [details of any supplementary information available should be included here]. See DOI: 10.1039/b000000x/

<sup>‡</sup> E-mail: joe.d.berry@gmail.com

<sup>¶</sup> E-mail: rrd@unimelb.edu.au

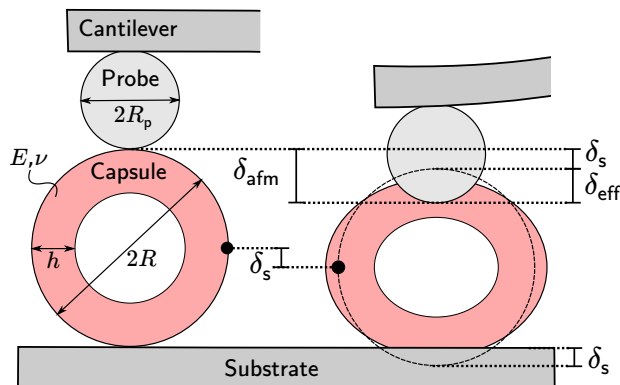


**Fig. 1** Schematic showing a typical experimental setup for the indentation of a capsule using Atomic Force Microscopy. A capsule of radius  $R$ , shell thickness  $h$ , Young's modulus  $E$ , and Poisson's ratio  $\nu$  is indented by a distance  $\delta_{\text{afm}}$  with a probe of radius  $R_p$  attached to a cantilever. The deflection of the cantilever is used to calculate the force  $F$  exerted on the capsule. The substrate on which the capsule rests indents the capsule by a distance  $\delta_s$ . The effective indentation experienced by the capsule can be calculated from  $\delta_{\text{eff.}} = \delta_{\text{afm}} - \delta_s$ , where  $\delta_s$  can be determined by measuring the distance moved by a point on the centreline of the capsule.

strate. As shown in Figure 1 the compression of a capsule or particle leads to deformation at both the top of the capsule or particle as well as at the bottom adjacent to the substrate. Thus, the indentation measured via the AFM cantilever deflection, designated as  $\delta_{\text{afm}}$ , is the sum of both the indentation caused by the substrate  $\delta_s$  and the *effective* indentation  $\delta_{\text{eff.}}$ . The AFM measurement alone does not provide sufficient information to separate the two components of the deflection. The substrate indentation  $\delta_s$  can be determined *a posteriori* by measuring the distance the capsule or particle moves during the indentation process (also  $\delta_s$ ), commonly by choosing a point along the centreline of the capsule or particle.

Using the effective indentation rather than the measured indentation in the analytical formulae of Hertz and Reissner gives the correct solution. Two examples of this are shown in Figure 2a) & b) for a thin-shell capsule and a solid particle respectively, calculated using a numerical simulation of the indentation process (see Supporting Information for further details of the numerical simulations). It is clear that both the capsule and the particle appear softer than they actually are if the measured indentation is used in the analysis. As a consequence, naïve application of Reissner or Hertz theory in the analysis of experimental force-indentation data results in significant under-estimation of shell and particle material properties. Correction factors that account for the substrate indentation have been derived analytically for soft micro-particles<sup>17</sup> ( $h/R = 1$ ), defined in terms of the indenter radius ratio  $R_p/R$  as

$$C = \frac{\delta_{\text{eff.}}}{\delta_{\text{afm}}} = \frac{[(R_p/R) + 1]^{\frac{1}{3}}}{[(R_p/R) + 1]^{\frac{1}{3}} + (R_p/R)^{\frac{1}{3}}}. \quad (3)$$

A derivation of this expression is included in the Supporting Information. However, correction factors for capsules ( $h < R$ ) are not amenable to theoretical analysis. Hence, in this communication

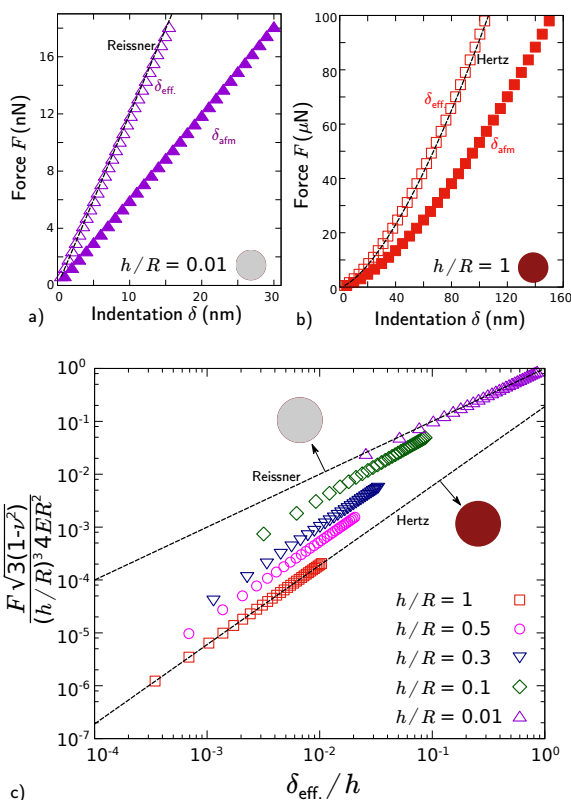


**Fig. 2** Applied force as a function of measured indentation  $\delta_{\text{afm}}$  (closed symbols) and effective indentation  $\delta_{\text{eff.}}$  (open symbols) for a) a thin capsule of radius  $R = 10 \mu\text{m}$  and shell thickness  $h = 100 \text{nm}$  ( $h/R = 0.01$ ) and b) a solid particle ( $h/R = 1$ ) of radius  $R = 10 \mu\text{m}$ . c) Normalised force-indentation curves for fixed indenter radius ratio  $R_p/R = 0.1$  for various values of shell thickness ratio  $h/R$ . The analytical solutions of Hertz (Equation 2) and Reissner (Equation 1) are shown with dashed lines. The material properties are Young's modulus  $E = 1.9 \text{GPa}$  and Poisson's ratio  $\nu = 0.4$ .

we use numerical simulations to characterise the correction factors required to calculate the effective indentation from the measured indentation over the range of shell thicknesses from thin shell capsules to solid particles, spanning the gap between the two limits of Reissner ( $h/R \ll 1$ ) and Hertz ( $h/R = 1$ ). In addition, we determine the appropriate variation of force with indentation necessary to obtain precise estimates of material properties.

It is important to recognise that Reissner and Hertz theories are solutions at the two opposite limits of the shell thickness ratio  $h/R$ . Indeed, the Reissner and Hertz formulae can be written in non-dimensional form as

$$\frac{F\sqrt{3(1-\nu^2)}}{(h/R)^3 4ER^2} = \begin{cases} \delta/h & \text{for } h/R \ll 1 \\ (\bar{R}/R)^{\frac{1}{2}} (\delta/h)^{\frac{3}{2}} & \text{for } h/R = 1 \end{cases} \quad (4)$$

Figure 2c) shows the transition from thin shell capsule indentation (Reissner solution) to solid particle indentation (Hertz solution) as  $h/R$  increases from  $10^{-2}$  to 1, for the indenter radius ratio  $R_p/R = 0.1$ .

We can rewrite Equation 4 in a more general, and more useful, form:

$$\frac{F\sqrt{3(1-\nu^2)}}{(h/R)^3 4R^2} = E\beta \left( \frac{C\delta_{\text{afm}}}{h} \right)^\alpha, \quad (5)$$

noting that Reissner's solution ( $h/R \ll 1$ ) gives  $\beta = 1$  and  $\alpha = 1$ , and, Hertz's solution ( $h/R = 1$ ) yields  $\beta = (\bar{R}/R)^{\frac{1}{2}} / \sqrt{3(1-\nu^2)}$  and  $\alpha = 3/2$ . Equation 5 can be used to calculate the Young's modulus of a capsule of arbitrary shell thickness ratio  $h/R$  from experimental force-indentation data, using appropriate values of the correction factor  $C$ , coefficient  $\beta$ , and scaling exponent  $\alpha$ . Through numerical simulation, we now proceed to outline how these (independent) parameters vary as functions of shell thickness ratio  $h/R$ , indenter radius ratio  $R_p/R$ , and Poisson's ratio  $\nu$ . We found that the Poisson's ratio had very little effect on the three parameters (Figure S3 in the Supporting Information). Consequently, for clarity we present the results for a fixed Poisson's ratio  $\nu = 0.4$ .

The correction factor  $C$  as a function of shell thickness ratio  $h/R$  is shown in Figure 3, for four different indenter radius ratios. Slight variation of the correction factor  $C$  was observed with increasing measured indentation  $\delta_{\text{afm}}$  (Figure S2 in the Supporting Information). The results here are presented for fixed normalised measured indentation  $\delta_{\text{afm}}/R = 0.05$ , with no loss of generality. The solid green line indicates the constant correction factor of  $C = 0.5$  for an indenter radius ratio  $R_p/R = \infty$ , corresponding to a symmetric compression between two parallel plates. The dashed lines depict the analytical solution for a solid particle ( $h/R = 1$ ) for the indenter radius ratios shown<sup>17</sup>. For small shell thickness ratios the correction factor is insensitive to the probe radius magnitude, in agreement with the independence of the Reissner theory to indenter radius. Interestingly, Reissner derived the relationship assuming a concentrated point load, but it has been shown that the theory is valid for any indenter radius<sup>18</sup>. For small shell thickness ratios the correction factor is of size  $C \sim 0.5$ . As  $h/R$  increases the indenter radius ratio begins to become important, and the correction factor increases above 0.5. For  $h/R = 1$  the simulation results match the analytical solution of Glaubitz *et al.*<sup>17</sup> for

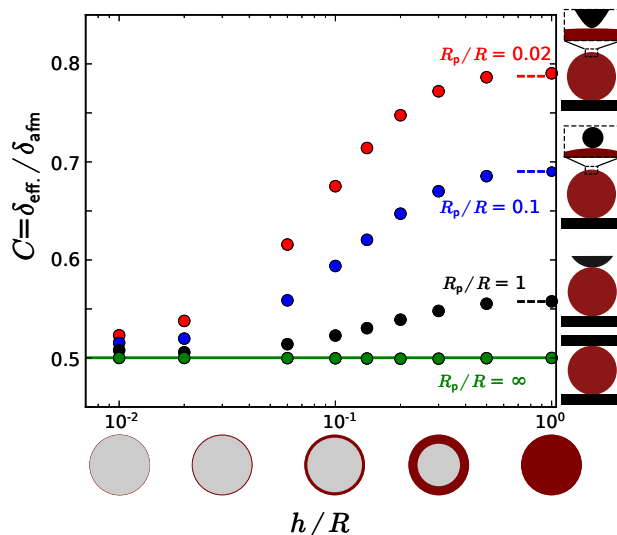
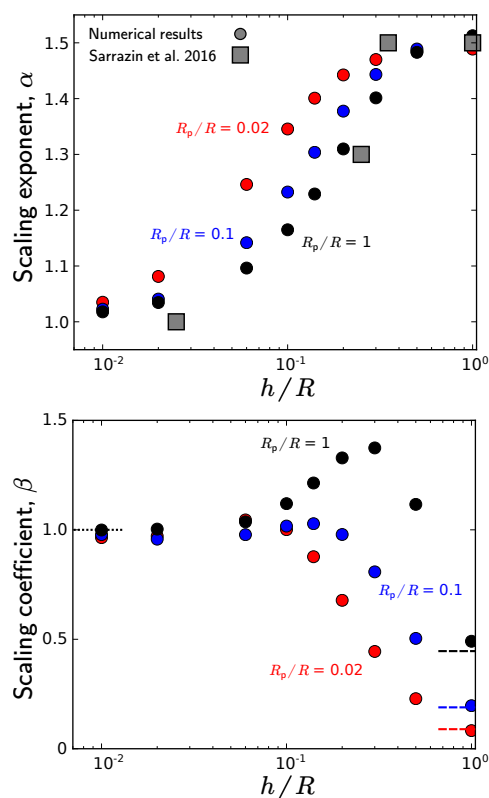


**Fig. 3** Correction factor  $C = \delta_{\text{eff}}/\delta_{\text{afm}}$  as a function of shell thickness ratio  $h/R$  for indenter radius ratios  $R_p/R = 0.02, 0.1, 1$ , and  $\infty$ . The solid green line indicates the constant correction factor of  $C = 0.5$  for  $R_p/R = \infty$ . The normalised measured indentation is  $\delta_{\text{afm}}/R = 0.05$ . The dashed lines at  $h/R = 1$  are the analytical solutions of Glaubitz *et al.*<sup>17</sup> (Equation 3) for solid particles for the indenter radius ratios depicted.

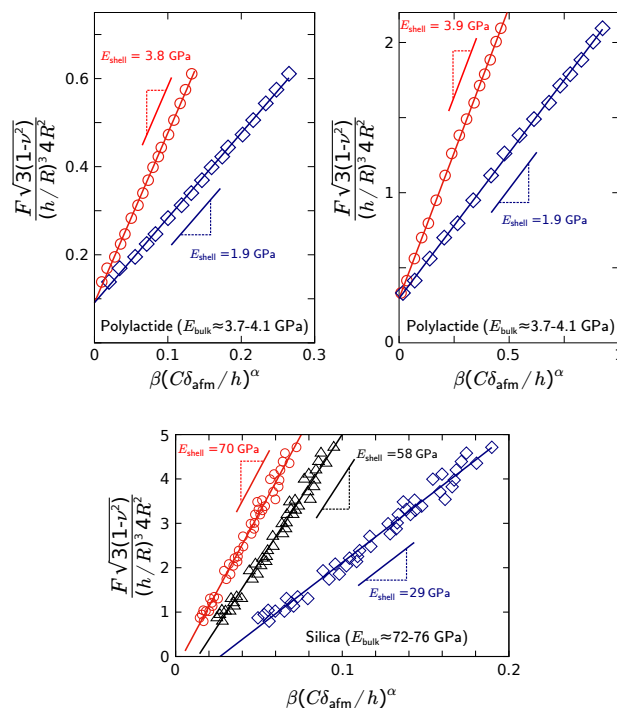
solid particles. An interesting observation is that the correction factor is sensitive to indenter radius ratios  $R_p/R \lesssim 1$ , but is close to the high indentation radius limit value of  $C = 0.5$  for indenter radius ratios greater than unity.

Figure 4 shows the variation of the coefficient  $\beta$  and the scaling exponent  $\alpha$  with shell thickness ratio  $h/R$ , for three different indenter radius ratios. Also shown are the experimental results of Sarrazin *et al.*<sup>19</sup>, measured using oil-filled polymer (poly(lactide-co-glycolide), PLGA) microcapsules. The scaling exponent  $\alpha$  increases monotonically from 1 to 1.5 as the shell thickness ratio increases from 0.01 to 1, in agreement with the two limits posited by Reissner and Hertz respectively, with slight dependence on the indenter radius ratio. Good agreement is also evident with the experimental results of Sarrazin *et al.*<sup>19</sup>. The coefficient  $\beta$  is  $\sim 1$  for shell thickness ratios  $R_p/R \lesssim 0.1$ , in agreement with the Reissner formula. At  $h/R = 1$ ,  $\beta$  approaches the Hertz solution, which is dependent upon the indenter radius ratio (and to a lesser extent the Poisson ratio). For a fixed shell thickness ratio above  $10^{-1}$ , the coefficient increases with increasing indenter radius ratio.

To validate our numerical calculations, in Figure 5 we show three examples of existing experimental force-indentation data from the literature, presented in the form given by Equation 5. The first two examples are polylactide capsules of different sizes and fixed shell thickness ratio  $h/R = 0.015$ , compressed between two flat plates ( $R_p/R = \infty$ ). Experimental parameters are listed in Table S1 in the Supporting Information. With the appropriate values of correction factor  $C$ , scaling coefficient  $\beta$ , and scaling exponent  $\alpha$ , chosen based on the geometry of the measurement, the measured Young's modulus of the shell agrees well with the established literature value of  $E \approx 3.7 - 4.1$  GPa<sup>22</sup>. The third example is a silica capsule with  $h/R = 0.06$ , compressed with a nano-indenter of radius  $< 20$  nm. Again, with the appropriate parame-



**Fig. 4** a) The scaling exponent  $\alpha$ , and b) the scaling coefficient  $\beta$ , as a function of shell thickness ratio  $h/R$  for three indenter radius ratios  $R_p/R = 0.02$  (red circles), 0.1 (blue circles) & 1 (black circles). The Poisson's ratio  $\nu = 0.4$ . The experimental results of Sarrazin *et al.*<sup>19</sup> are also shown with grey squares ( $R_p/R \approx 0.04 - 0.1$ ,  $\nu = 0.33$ ). The dotted line in b) indicates Reissner's solution  $\beta = 1$  and the dashed lines indicate the Hertz solution  $\beta = (\bar{R}/R)^{1/2} / \sqrt{3(1-\nu^2)}$  for each indenter radius ratio depicted.



**Fig. 5** Experimental validation using the data of Glynos *et al.*<sup>20</sup> and Zhang *et al.*<sup>21</sup> for poly lactide and silica capsules respectively. The blue symbols represent the uncorrected indentation data fitted using Reissner's equation, and the red symbols represent the corrected indentation data, calculated using Equation 5. The fitting parameters used are: a) & b)  $\beta = 0.636$ ,  $\alpha = 1$ ,  $C = 0.5$ , and c)  $\beta = 0.52$ ,  $\alpha = 1.2$ ,  $C = 0.6$ . The black symbols in c) represent the fit used in Zhang *et al.*<sup>21</sup> (Reissner's formula with a correction factor of  $C = 0.5$ ). The experimental parameters are given in Table S1 and the raw data is shown in Figure S4 in the Supporting Information.

ters, Equation 5 gives an accurate measurement of Young's modulus in comparison to the established value of  $E \approx 72 - 76 \text{ GPa}$ <sup>23</sup>. Notably, Zhang *et al.*<sup>21</sup> do account for the indentation due to the substrate when fitting the experimental data using Reissner's theory, albeit with a correction factor  $C = 0.5$  instead of the correct value of  $C = 0.6$ .

We have demonstrated conclusively that analysis of experimental data of capsule and particle compression under-predicts material properties such as the Young's modulus by up to 100% if the indentation due to the presence of the rigid substrate is not taken into account. Counter-intuitively, if the effect of the substrate is not accounted for, indentation of particles and capsules against a substrate leads to an underestimation of the material properties, in contrast to the overestimation of material properties during indentation of thin films<sup>24</sup>.

Through systematic numerical calculations over the parameters of shell thickness ratio  $h/R$ , indenter radius ratio  $R_p/R$  and Poisson's ratio  $\nu$ , we characterise the correction factors required to calculate the effective indentation from the measured indentation, and determine the appropriate variation of force with indentation necessary to obtain precise estimates of material properties. The analysis presented is based upon idealised behaviour of the capsule, with homogeneous material properties and uniform wall thickness. In practice imperfections in shell thickness and material properties will be present, however the effect of these imperfections on the correction factor will be minimal due to the narrow range of values possible,  $0.5 \leq C \leq 1$ , over the entire parameter space. Importantly, the analysis presented relies upon accurate measurements of shell thicknesses, and indentations less than the shell thickness (and much smaller than the particle radius), in order to obtain accurate material properties.

In capsule or particle compression studies where relative trends in stiffness or modulus have been measured<sup>25</sup>, the implications of the outcomes of this study are unlikely to affect the qualitative trends for similarly sized capsules or particles with similar shell thickness. However, studies where comparisons are made with disparate capsule or particle size or shell thickness<sup>26</sup>, or in comparison between a modulus obtained using AFM to a modu-

lus measured via different techniques, the analysis presented here is expected to be critical. In the Supporting Information we provide tables and a simple MATLAB calculator giving the necessary parameters for the accurate calculation of Young's modulus for a given experimental setup.

Future work will focus on the effect that adhesion between the capsule and the indenter, and between the capsule and the substrate, has on the accuracy of the measurement.

## References

- 1 G. Riccati, *Mem. Mat. Fis. Soc. Italiana*, 1782, **1**, 444–525.
- 2 I. Sneddon, *Int. J. Eng. Sci.*, 1965, **3**, 47–57.
- 3 Y.-T. Cheng and C.-M. Cheng, *Mat. Sci. Eng. R*, 2004, **44**, 91–149.
- 4 B. Cappella and G. Dietler, *Surf. Sci. Rep.*, 1999, **34**, 1–104.
- 5 H.-J. Butt, B. Cappella and M. Kappl, *Surf. Sci. Rep.*, 2005, **59**, 1–152.
- 6 A. E. Pelling, S. Sehati, E. B. Gralla, J. S. Valentine and J. K. Gimzewski, *Science*, 2004, **305**, 1147–1150.
- 7 S. Tan, R. L. Sherman and W. T. Ford, *Langmuir*, 2004, **20**, 7015–7020.
- 8 A. Fery, F. Dubreuil and H. Möhwald, *New J. Phys.*, 2004, **6**, 18.
- 9 A. P. Esser-Kahn, S. A. Odom, N. R. Sottos, S. R. White and J. S. Moore, *Macromolecules*, 2011, **44**, 5539–5553.
- 10 S. E. Cross, Y.-S. Jin, J. Rao and J. K. Gimzewski, *Nat. Nanotechnol.*, 2007, **2**, 780–783.
- 11 D. E. Discher, P. Janmey and Y.-I. Wang, *Science*, 2005, **310**, 1139–1143.
- 12 A. Schneider, G. Francius, R. Obeid, P. Schwinte, J. Hemmerle, B. Frisch, P. Schaaf, J.-C. Voegel, B. Senger and C. Picart, *Langmuir*, 2006, **22**, 1193–1200.
- 13 T. J. Merkel, S. W. Jones, K. P. Herlihy, F. R. Kersey, A. R. Shields and M. Napier, *Proc. Natl. Acad. Sci. USA*, 2011, **108**, 586–591.
- 14 E. Reissner, *J. Math. Phys.*, 1947, **25**, 279–300.
- 15 H. Hertz, *Journal für die reine und angewandte Mathematik*, 1882, **92**, 156–171.
- 16 F. Y. M. Wan, R. D. Gregory and T. I. Milac, *SIAM J. Appl. Math.*, 1998, **59**, 1080–1097.
- 17 M. Glaubitz, N. Medvedev, D. Pussak, L. Hartmann, S. Schmidt, C. A. Helm and M. Delcea, *Soft Matter*, 2014, **10**, 6732–6741.
- 18 N. Elsner, F. Dubreuil, R. Weinkamer, M. Wasicek, F. D. Fischer and A. Fery, *Prog. Colloid Polym. Sci.*, 2006, **132**, 117–123.
- 19 B. Sarrazin, N. Tsapis, L. Mousnier, N. Taulier, W. Urbach and P. Guenoun, *Langmuir*, 2016, 4610–4618.
- 20 E. Glynos, V. Koutsos, W. N. McDicken, C. M. Moran, S. D. Pye, J. A. Ross and V. Sboros, *Langmuir*, 2009, **25**, 7514–7522.
- 21 L. Zhang, M. D. Acunzi, M. Kappl, A. Imhof, D. Vollmer and A. V. Blaaderen, *Phys. Chem. Chem. Phys.*, 2010, **12**, 15392–15398.
- 22 D. Garlotta, *J. Polym. Environ.*, 2002, **9**, 63–84.
- 23 T. Adachi and S. U. M. I. O. Sakka, *J. Mater. Sci.*, 1990, **25**, 4732–4737.
- 24 E. K. Dimitriadis, F. Horkay, J. Maresca, B. Kachar and R. S. Chadwick, *Biophys. J.*, 2002, **82**, 2798–2810.
- 25 S. Mettu, M. Zhou, B. L. Tardy, M. Ashokkumar and R. R. Dagastine, *Polymer*, 2016, **102**, 333–341.
- 26 S. Tan, S. Mettu, M. D. Biviano, M. Zhou, B. Babji, J. White, R. R. Dagastine and M. Ashokkumar, *Soft Matter*, 2016, **12**, 7212–7222.

# Precise measurements of capsule mechanical properties using indentation

Joseph D. Berry,<sup>1,2,\*</sup> Srinivas Mettu,<sup>1,2</sup> and Raymond R. Dagastine<sup>1,2,†</sup>

<sup>1</sup>*Department of Chemical and Biomolecular Engineering,  
University of Melbourne, Parkville, Victoria 3010, Australia*

<sup>2</sup>*Particulate Fluids Processing Centre,  
University of Melbourne, Parkville Victoria, 3010, Australia*

(Dated: February 13, 2017)

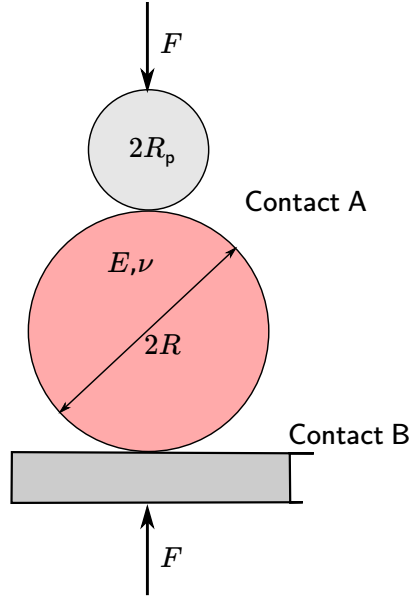


FIG. S1. Schematic of the two contact problem for a particle.

## SUPPLEMENTAL MATERIAL

### Derivation of correction factor expression for microparticle compression

For sufficiently soft particles, the correction factor is a function of the indenter radius ratio, as shown by Glaubitz *et al.* [1] for the particle case ( $h/R = 1$ ). To elucidate this further, consider a solid particle of radius  $R$ . Hertz theory shows that the force on a particle due to indentation is linearly proportional to the contact radius and the indentation depth. Thus, for a fixed force, increasing the contact radius will decrease the indentation depth, and vice versa. In the particle reference frame, we have a spherical probe of radius  $R_p$  indenting the top of the particle, and the flat substrate indenting the bottom of the particle (Figure S1). If the correction factor  $C$  is equal to 0.5, then the indentation depths at the top and the bottom of the particle will be equal. However, it is clear that the contact areas (and thus contact radii) at the top and the bottom of the particle are not equal (unless the probe and the substrate have the same radii). Further, the forces acting at the top and the bottom of the particle are equal and opposite, meaning that the indentation depth at the top must be greater than the indentation depth at the bottom due to the difference in contact radii of the probe and the substrate. Consequently, the correction factor is not always 0.5, rather it is a function of the indenter radius ratio, even if the probe and substrate are stiff compared

to the particle.

The relationship between correction factor and indenter radius ratio can be analytically derived as follows. In the reference frame of the particle, the probe indents the particle by a distance  $\delta_A$  and the substrate indents the particle by a distance  $\delta_B$ . The force  $F$  is equal and opposite for contact A & B, and can be defined using the Hertz equation as:

$$F = \frac{4E\bar{R}_A^{\frac{1}{2}}\delta_A^{\frac{3}{2}}}{3(1-\nu^2)} \quad (\text{Contact A}) \quad (\text{S1})$$

$$F = \frac{4E\bar{R}_B^{\frac{1}{2}}\delta_B^{\frac{3}{2}}}{3(1-\nu^2)} \quad (\text{Contact B}) \quad (\text{S2})$$

Combining equations S1 & S2 gives:

$$\bar{R}_A^{\frac{1}{2}}\delta_A^{\frac{3}{2}} = \bar{R}_B^{\frac{1}{2}}\delta_B^{\frac{3}{2}} \quad (\text{S3})$$

Thus, the indentation due to the substrate  $\delta_B$  can be written in terms of the indentation due to the particle  $\delta_A$  with:

$$\delta_B = \left(\frac{\bar{R}_A}{\bar{R}_B}\right)^{\frac{1}{3}} \delta_A \quad (\text{S4})$$

In the laboratory reference frame the substrate is fixed in place and no indentation occurs, whilst the probe indents the particle by a distance  $\delta_A + \delta_B$ . Using the notation of Figure 1 in the manuscript, this distance is the measured indentation  $\delta_{\text{afm}}$ , and  $\delta_A$  and  $\delta_B$  are  $\delta_{\text{eff}}$  and  $\delta_s$  respectively. Thus:

$$\delta_{\text{afm}} = \delta_{\text{eff}} + \delta_s = \delta_{\text{eff}} + \left(\frac{\bar{R}_A}{\bar{R}_B}\right)^{\frac{1}{3}} \delta_{\text{eff}} = \delta_{\text{eff}} \left[1 + \left(\frac{\bar{R}_A}{\bar{R}_B}\right)^{\frac{1}{3}}\right] \quad (\text{S5})$$

Because the substrate is flat the effective radius  $\bar{R}_B = R$ , where  $R$  is the radius of the particle. Further, the effective radius  $\bar{R}_A = R_p R / (R_p + R)$ , where  $R_p$  is the radius of the probe. Thus, Equation S5 becomes:

$$\delta_{\text{afm}} = \delta_{\text{eff}} \left[1 + \left(\frac{R_p}{R_p + R}\right)^{\frac{1}{3}}\right] \quad (\text{S6})$$

and the correction factor  $C$  can be written as:

$$C = \frac{\delta_{\text{eff}}}{\delta_{\text{afm}}} = \left[1 + \left(\frac{R_p}{R_p + R}\right)^{\frac{1}{3}}\right]^{-1} \quad (\text{S7})$$

or, as a function of the indenter radius ratio  $R_p/R$  as:

$$C = \frac{\delta_{\text{eff}}}{\delta_{\text{afm}}} = \frac{[(R_p/R) + 1]^{\frac{1}{3}}}{[(R_p/R) + 1]^{\frac{1}{3}} + (R_p/R)^{\frac{1}{3}}}. \quad (\text{S8})$$

This result is consistent with the derivation in Glaubit *et al.* [1].



## Numerical method

The commercial software Comsol Multiphysics (5.2a) was used to carry out numerical simulations of the indentation process. Briefly, the capsule is in mechanical equilibrium, which is expressed mathematically as:

$$\partial_i \sigma_{ij} = 0, \quad (\text{S9})$$

where  $\boldsymbol{\sigma}$  is the stress tensor. Assuming that the behaviour of the material is linearly elastic, the constitutive relationship between stresses  $\sigma_{ij}$  and strains  $\epsilon_{ij}$  is given by Hooke's law:

$$\sigma_{ij} = \frac{E}{1 + \nu} \left[ \epsilon_{ij} + \frac{\nu}{1 - 2\nu} \epsilon_{kk} \delta_{ij} \right], \quad (\text{S10})$$

with  $E$  and  $\nu$  the capsule Young's modulus and Poisson's ratio respectively. The strains are defined in terms of the material displacement  $\mathbf{u}$  as

$$\epsilon_{ij} = \frac{1}{2} \left( \frac{\partial u_i}{\partial x_j} + \frac{\partial u_j}{\partial x_i} \right) \quad (\text{S11})$$

Figure S2 shows an example of the axisymmetric geometry and mesh used to solve equation S9 for the unknown material displacements  $\mathbf{u}$ . The indenter and the rigid substrate were each specified as a material with Young's modulus  $E_0 \gg E$ . The indenter was set to move with prescribed displacement  $\delta_{\text{afm}}$ , and the substrate was fixed in position. The subsequent movement of the capsule centreline  $\delta_s$  was measured, as well as the force  $F$  exerted on the indenter. The mesh size was typically 130,000 elements, with appropriate refinement near the indentation regions (Figure S2).

The capsule was set to a nominal radius of 10  $\mu\text{m}$ , and a nominal Young's modulus of 1.9 GPa. The indenter radius and shell thickness were then specified according to the values of  $R_p/R$  and  $h/R$  being investigated. The resulting displacements  $\delta_s$  and forces  $F$  were measured for indenter displacements in the nominal nanometre range  $0 < \delta_{\text{afm}} < \min(150, 0.5h)$ , giving a non-dimensional range of  $0 < \delta_{\text{afm}}/R < \min(0.015, 0.5h/R)$ . The resulting effective indentation  $\delta_s$  was not quite a linear function of the applied indentation  $\delta_{\text{afm}}$  (Figure S3). The correction factors plotted in the main text are taken for fixed normalised applied indentation  $\delta_{\text{afm}}/R = 0.05$ , indicated in red on Figure S3.

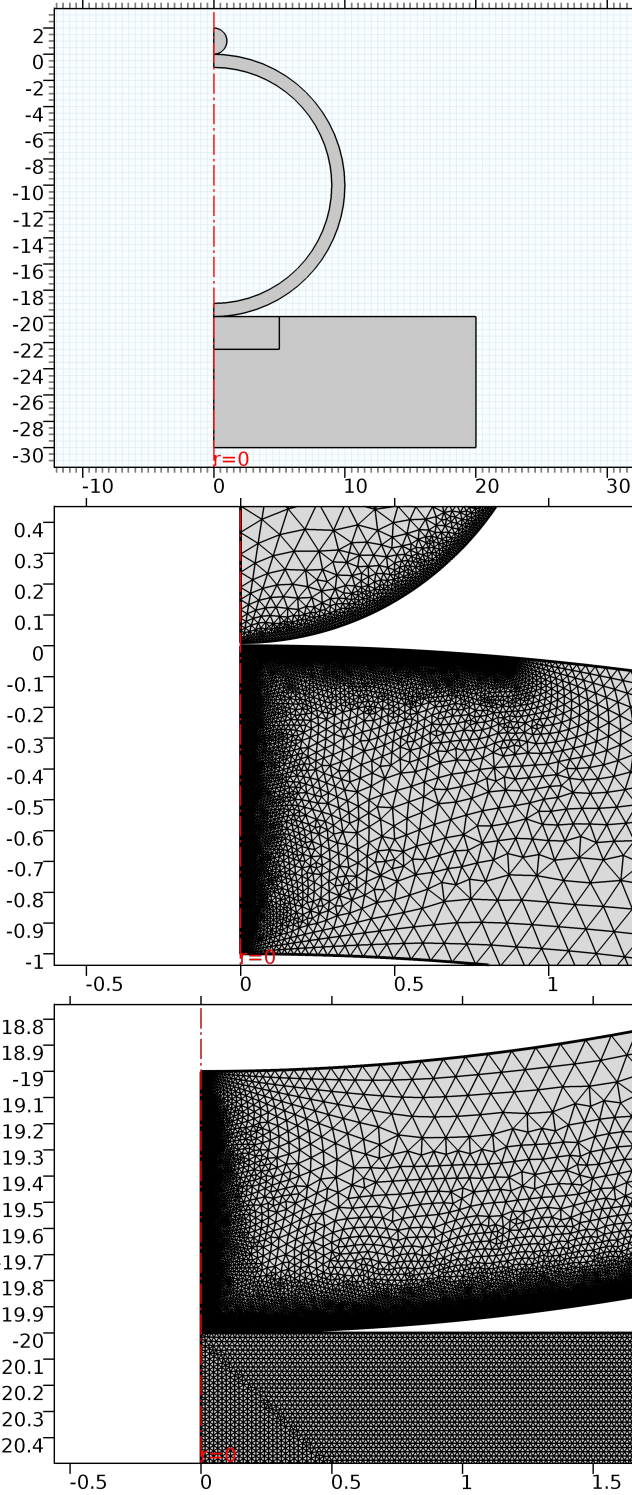
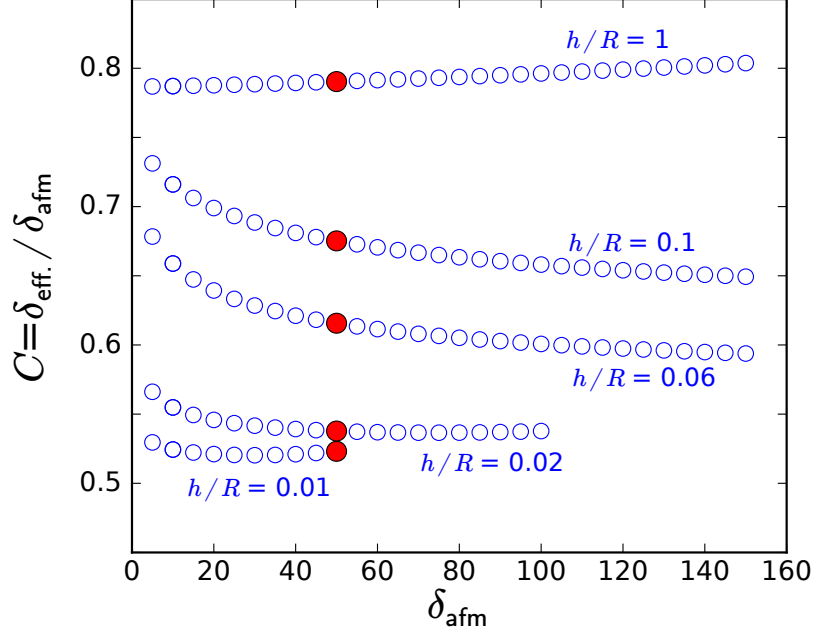
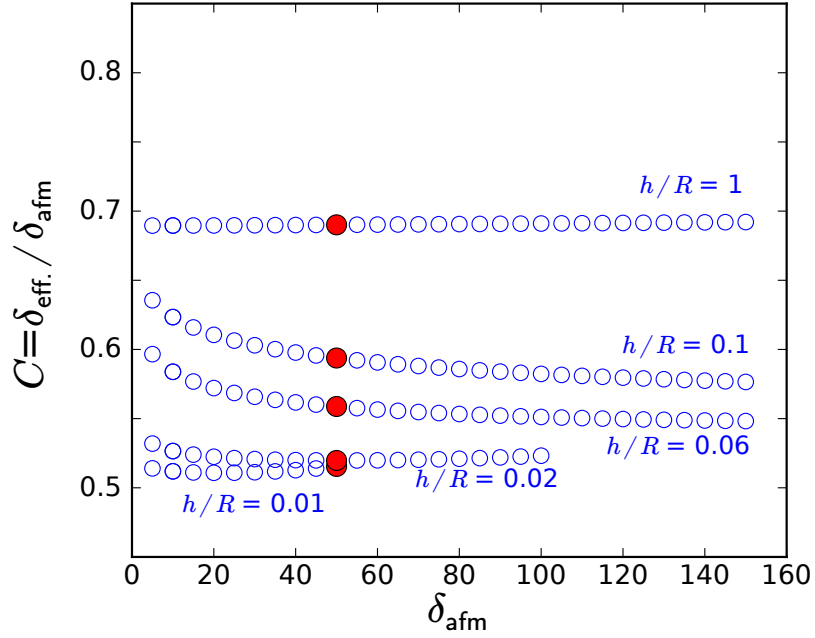


FIG. S2. Example of indenter, capsule & substrate geometry and mesh for indenter radius ratio  $R_p/R = 0.1$  and shell thickness ratio  $h/R = 0.1$ .



a)  $R_i/R = 0.02$



b)  $R_i/R = 0.1$

FIG. S3. Variation of correction factor  $C = \delta_{\text{eff.}} / \delta_{\text{afm}}$  with applied indentation  $\delta_{\text{afm}}$  for indenter radius ratios a)  $R_p/R = 0.02$ , and b)  $R_p/R = 0.1$ . The red symbols indicate the correction factors used in Figure 3, for fixed applied indentation of 50 nm ( $\delta_{\text{afm}}/R = 0.005$ ).

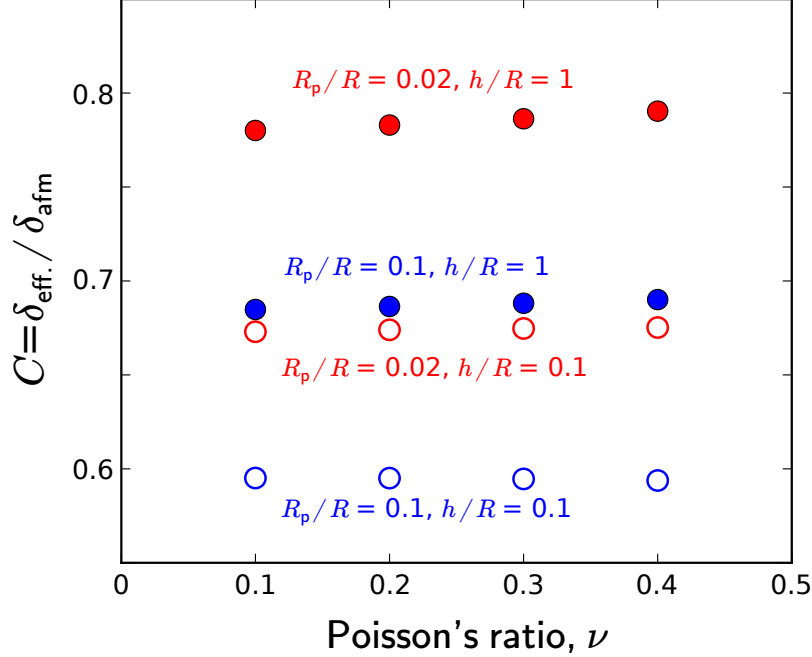


FIG. S4. Variation of correction factor  $C = \delta_{\text{eff.}}/\delta_{\text{afm}}$  with Poisson's ratio  $\nu$  for different shell thickness and indenter radius ratios.

TABLE S1. Experimental parameters for the capsule data shown in Figures 5 & S5.

Figure	Material	$\nu$	R ( $\mu\text{m}$ )	h (nm)	$R_p$ (nm)	$h/R$	$R_p/R$
5c)	Silica [2]	0.17	0.905	52	$\lesssim 20$	0.06	$\lesssim 0.02$
5a)	Poly lactide [3]	0.42	1.25	19	$\infty$	0.015	$\infty$
5b)	Poly lactide [3]	0.42	2.4	36	$\infty$	0.015	$\infty$

### Interpolation tables and MATLAB calculator

In order to accurately determine the Young's modulus  $E$  from experimental force-indentation data, the data needs to be rescaled using Equation 5 in the manuscript:

$$\frac{F\sqrt{3(1-\nu^2)}}{(h/R)^3 4R^2} = E\beta \left( \frac{C\delta_{\text{afm}}}{h} \right)^\alpha. \quad (\text{S12})$$

The parameters  $C$ ,  $\alpha$  &  $\beta$  are functions of the experimental parameters Poisson's ratio  $\nu$ , the indenter radius ratio  $R_p/R$ , and the shell thickness ratio  $h/R$ . Interpolation tables for the correction parameter  $C$  are presented as functions of shell thickness ratio and indenter radius ratio in Tables 1A - 1D for Poisson's ratios of  $\nu = 0.1 - 0.4$  respectively. Similarly, Tables 2A

- 2D present the scaling exponent  $\alpha$ , and Tables 3A - 3D present the scaling exponent  $\beta$ , for each Poisson's ratio simulated. Note that the data is presented in terms of the logarithms of  $h/R$  and  $R_p/R$ . A MATLAB calculator is also included in the .zip file associated with this ESI that will generate appropriate parameters for a specific experimental dataset.

---

\* joe.d.berry@gmail.com

† rrd@unimelb.edu.au

- [1] M. Glaubitz, N. Medvedev, D. Pussak, L. Hartmann, S. Schmidt, C. A. Helm, and M. Delcea, *Soft Matter* **10**, 6732 (2014).
- [2] L. Zhang, M. D. Acunzi, M. Kappl, A. Imhof, D. Vollmer, and A. V. Blaaderen, *Phys. Chem. Chem. Phys.* **12**, 15392 (2010).
- [3] E. Glynos, V. Koutsos, W. N. McDicken, C. M. Moran, S. D. Pye, J. A. Ross, and V. Sboros, *Langmuir* **25**, 7514 (2009).

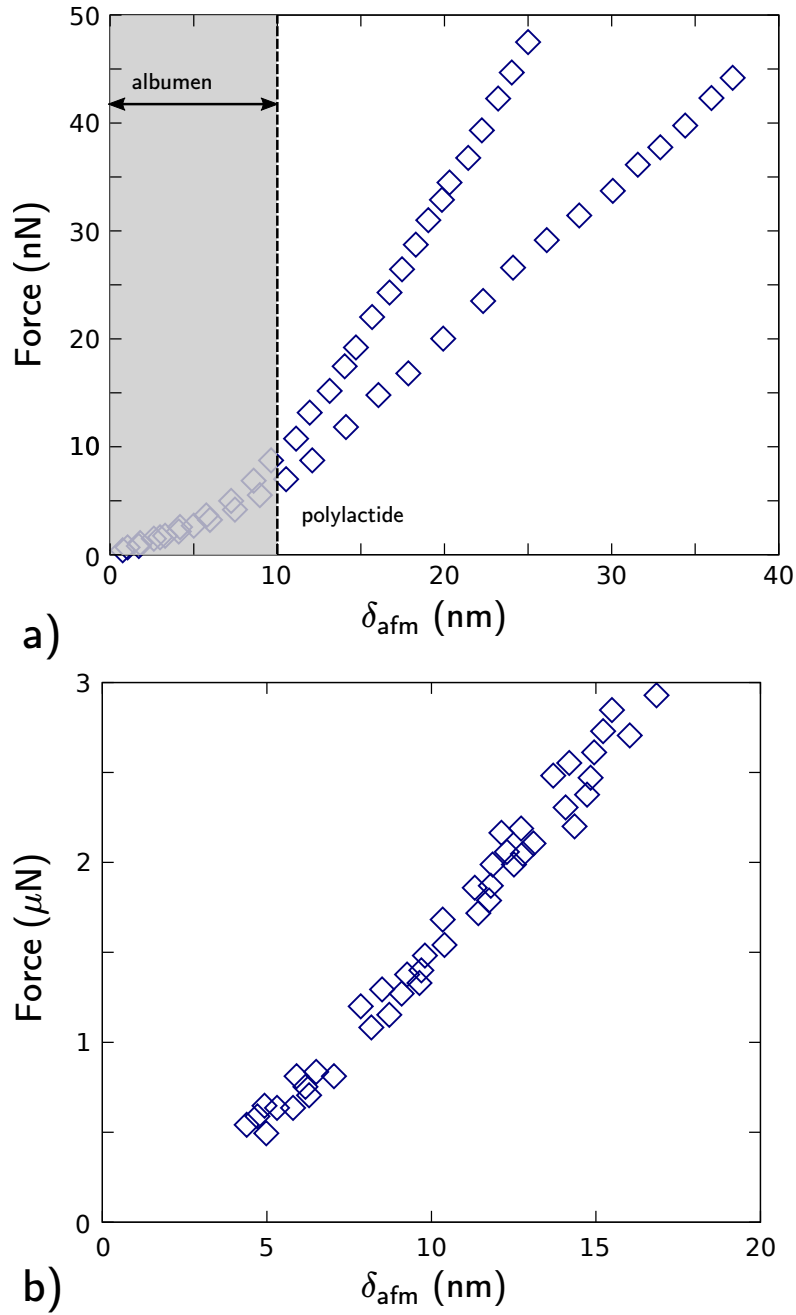


FIG. S5. Raw experimental data of a) Glynos *et al.* [3] and b) Zhang *et al.* [2]. The experimental parameters are listed in Table S1. The polylactide capsules are covered in a 10 nm thick layer of albumen, and consequently the data within the first 10 nm is not used in the calculation of the Young's modulus for polylactide.































Minerva Access is the Institutional Repository of The University of Melbourne

**Author/s:**

Berry, JD; Mettu, S; Dagastine, RR

**Title:**

Precise measurements of capsule mechanical properties using indentation

**Date:**

2017-03-14

**Citation:**

Berry, J. D., Mettu, S. & Dagastine, R. R. (2017). Precise measurements of capsule mechanical properties using indentation. *SOFT MATTER*, 13 (10), pp.1943-1947.  
<https://doi.org/10.1039/c6sm02841a>.

**Persistent Link:**

<http://hdl.handle.net/11343/243036>

**File Description:**

Accepted version